NOAA Technical Memorandum ERL SEL-25

U.S. DEPARTMENT OF COMMERCE
NATIONAL OCEANIC AND ATMOSPHERIC ADMINISTRATION
Environmental Research Laboratories

Initial Explorer 45 Substorm Observations and Electric Field Considerations

DONALD J. WILLIAMS
JOSEPH N. BARFIELD
THEODORE A. FRITZ

Space
Environment
Laboratory
BOULDER,
COLORADO
July 1973

ONMENTAL RESEARCH LABORATORIES

SPACE ENVIRONMENT LABORATORY

NATIONAL OCEANIC AND ATMOSPHERIC ADMINISTRATION

BOULDER, COLORADO

U.S. DEPARTMENT OF COMMERCE
National Oceanic and Atmospheric Administration
Environmental Research Laboratories

NOAA Technical Memorandum ERL SEL-25

INITIAL EXPLORER 45 SUBSTORM OBSERVATIONS AND ELECTRIC FIELD CONSIDERATIONS

Donald J. Williams
Space Environment Laboratory

Joseph N. Barfield
Environmental Data Service

Theodore A. Fritz
Space Environment Laboratory

Space Environment Laboratory
Boulder, Colorado
July 1973

TABLE OF CONTENTS

ABSTRACT

We present initial Explorer 45 substorm observations of particle distributions near the equator at altitudes of 5 to 5.5 earth radii. These results pertain to the evening sector and to a substorm occurring at 2200 ± 10 UT on December 12, 1971. Fluxes, spectra, and energy densities are presented for protons ($1 \leq E_p \leq 300$ keV) and electrons ($1.5 \leq E_e \leq 560$ keV). Arrival time dispersion effects are shown for electrons but not for protons, because proton intensities began their substorm response while Explorer 45 was still within the plasmasphere. These data are compared with the plasma cloud concepts and electric field model used by DeForest and McIlwain (1971) and McIlwain (1972) to explain particle observations at geosynchronous orbit. The plasma cloud concept is consistent with these observations in the sense that a static electric field is unable to flow particles in a continuous manner from the plasma sheet to the Explorer 45 location. A discontinuous change, perhaps in the $\overline{E}$ and $\overline{B}$ field configuration, is required to place substorm associated particles (plasma clouds) at low altitudes at the initiation of the substorm. Following this short-lived injection, the fields return to more or less normal values which govern the subsequent motion of the injected particles. From this data, we can infer an outward radial component in the equatorial electric field at L = 5.5 and ∿ 2100 hours LT of magnitude 0.81 ± 0.16 mV/m in a corotating coordinate system (0.33 ± 0.16 mV/m in a fixed coordinate system). Analysis of ATS-5 data during the same substorm yields an electric field radial component of magnitude 0.32 ± 0.03 mV/m in a corotating system (0.0 ± 0.03 mV/m in a fixed system) at L ∿ 6.8 and 1700 hours LT.

INITIAL EXPLORER 45 SUBSTORM OBSERVATIONS AND ELECTRIC FIELD CONSIDERATIONS

Donald J. Williams
Space Environment Laboratory

Joseph N. Barfield
Environmental Data Service

and

Theodore A. Fritz
Space Environment Laboratory

1. INTRODUCTION

We present here the initial results of a study to determine the behavior of the magnetospheric particle population during substorms at altitudes significantly within geosynchronous orbit. Previous studies in the geosynchronous orbit have shown effects of particle injection and acceleration (Parks and Winckler, 1968; Arnoldy and Chan, 1969; Lezniak and Winckler, 1970) along with effects of drift in the geomagnetic and geoelectric field (McIlwain, 1972; Shelley et al., 1971; DeForest and McIlwain, 1971; Winckler, 1970). A question still remains about how far into the trapping regions these effects appear and what additional effects need to be accounted for to maintain the particle population within the inner magnetosphere.

The long-term approach of this study is to identify times when substorms occurred while Explorer 45 was at or near its apogee. During these periods, the best opportunity exists to attempt to separate spatial and temporal effects. Spatial motion still occurs at apogee, however,

since the satellite drifts in longitude. A statistical study of particle behavior during all substorms satisfying this criterion is also being conducted.

The results presented here are from a single substorm that occurred late on December 12, 1971. These data are a good example of those obtained from Explorer 45 during substorms, and the presentation and discussion will indicate the approach taken in studying substorms and their effects at these altitudes.

2. DATA

The primary data for this study were collected by a set of particle detectors aboard Exporer 45, which was launched on November 15, 1971, into an elliptical orbit having an apogee of 5.24 earth radii, a perigee of 220 km, a period of 7.82 hours, and an inclination of 3.5°. Low-energy proton and electron intensities are obtained from an electrostatic analyzer-channeltron instrument that measures from 0.73 keV to 30.23 keV in 16 energy intervals. Higher energy electron information is obtained from a magnetic spectrometer using an 800 G magnet and four rectangular surface barrier solid-state detectors. The energy intervals measured are 35 to 70 keV, 75 to 125 keV, 120 to 240 keV, and 240 to 560 keV. Higher energy proton intensities are obtained via a telescope detector system consisting of two surface barrier solid-state detectors behind a 2.2 kG magnet used to sweep out electrons of 300 keV. Six energy intervals are obtained for protons in the range 24 keV to 300 keV. This latter instrument is affected by amplifier saturation in the presence of high energy ($\geq$ 1 MeV) protons. The nature of this effect and the checks for normal operation have been described previously (Williams et al., 1973). A detailed description of this effect and methods to determine normal operation is in preparation. The data presented here for the substorm analysis have been inspected and do not show signs of any saturation.

2.1 Substorm Timing

The substorm onset time was determined by examining auroral zone magnetic records from observatories in the nightside region. Figure 1 shows magnetograms from Sodankyla (2250 LT) and Abisko (2213 LT), which were near local midnight when a substorm started at approximately 2200 UT, December 12, 1971. The signature recorded at each observatory was typical of that seen at a midnight station (Akasofu, 1968). The initial, sharp decrease in the H-components together with the start of the rapid variations in the D-component suggest that the substorm may have begun as early as 2150 UT or as late as 2210 UT. We therefore shall use a start time of 2200 ± 10 UT.

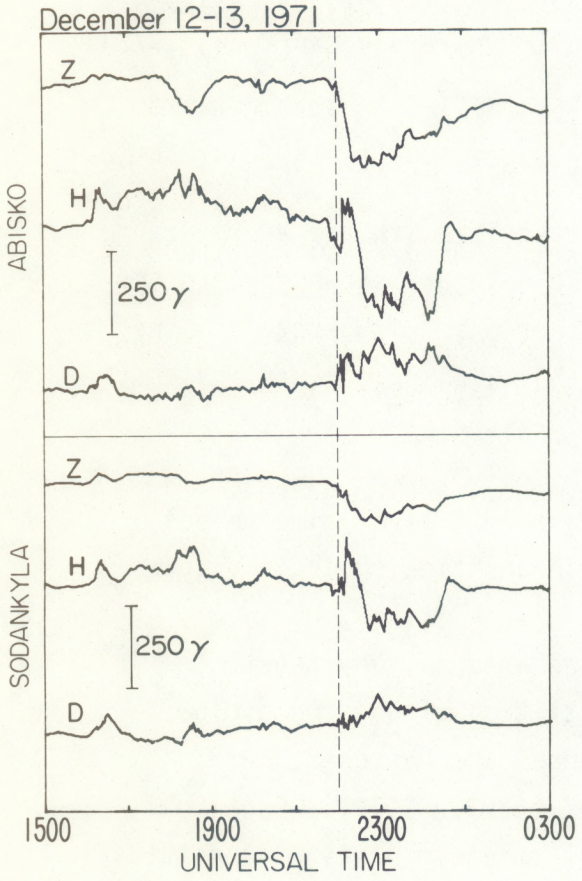

Figure 1. Ground magnetograms from the high latitude observatories Sodankyla and Abisko for 1500 UT, December 12 to 0300 UT December 13, 1971. At 2200 UT, LT for Abisko was 2213 and for Sodankyla 2250.

A wide longitude interval apparently was involved in this substorm since it was observed at Great Whale River (1650 LT), Leirvogur (2100 LT), Dixon Island (0320 LT), and Tixie Bay (0640 LT) as well as the stations shown in figure 1.

The substorm that occurred at 2200 ± 10 UT was preceded by moderate substorm activity that ended at ∿ 1900 UT. Thus, it is possible that the flux variations discussed in this paper were influenced to some extent by earlier activity. However, the 3 hours before the substorm at 2150 UT were relatively quiet, and the influence of the earlier one would be expected to be secondary.

The substorm occurred while Explorer 45 was near apogee of orbit 86. The trajectory of the satellite is given in figure 2. The substorm began as the satellite was outbound, at L = 5.3 and near 2040 LT. A short time later, as the substorm progressed the satellite passed outward through the plasmapause at 2221 UT, as indicated by saturation of the d-c electric field experiment on-board (Maynard and Cauffman, 1973). Its re-entry of the plasmapause occurred at ∿ 0039 UT.

2.2 Proton Observations

Figures 3 and 4 show proton flux intensities in the energy range 1.01 to 300 keV as a function of time. The data are shown for protons with 90° local pitch angle. Time of substorm onset is denoted by the vertical dashed line labeled "SS." Note that Explorer 45 was inside the plasmapause when the first protons possibly associated with the substorm appeared.

For three reasons, we hesitate to assign arrival time versus energy values to the substorm-associated intensities shown in figures 3 and 4.

1. Proton fluxes are possibly attenuated as they penetrate the plasmapause due to the initiation of the ion cyclotron resonance interaction (Kennel and Petschek, 1966; Cornwall et al., 1970; Williams et al., 1973). Because of this possibility, the actual substorm proton intensities may not be the values observed; thus, the relative times

when various energy thresholds show increases may not actually be relative arrival times.

2. Although L changes by a very small amount during the initial rise (figs. 3 and 4), we may be seeing a partial spatial effect similar to "nose" events discussed by Smith and Hoffman (1973).

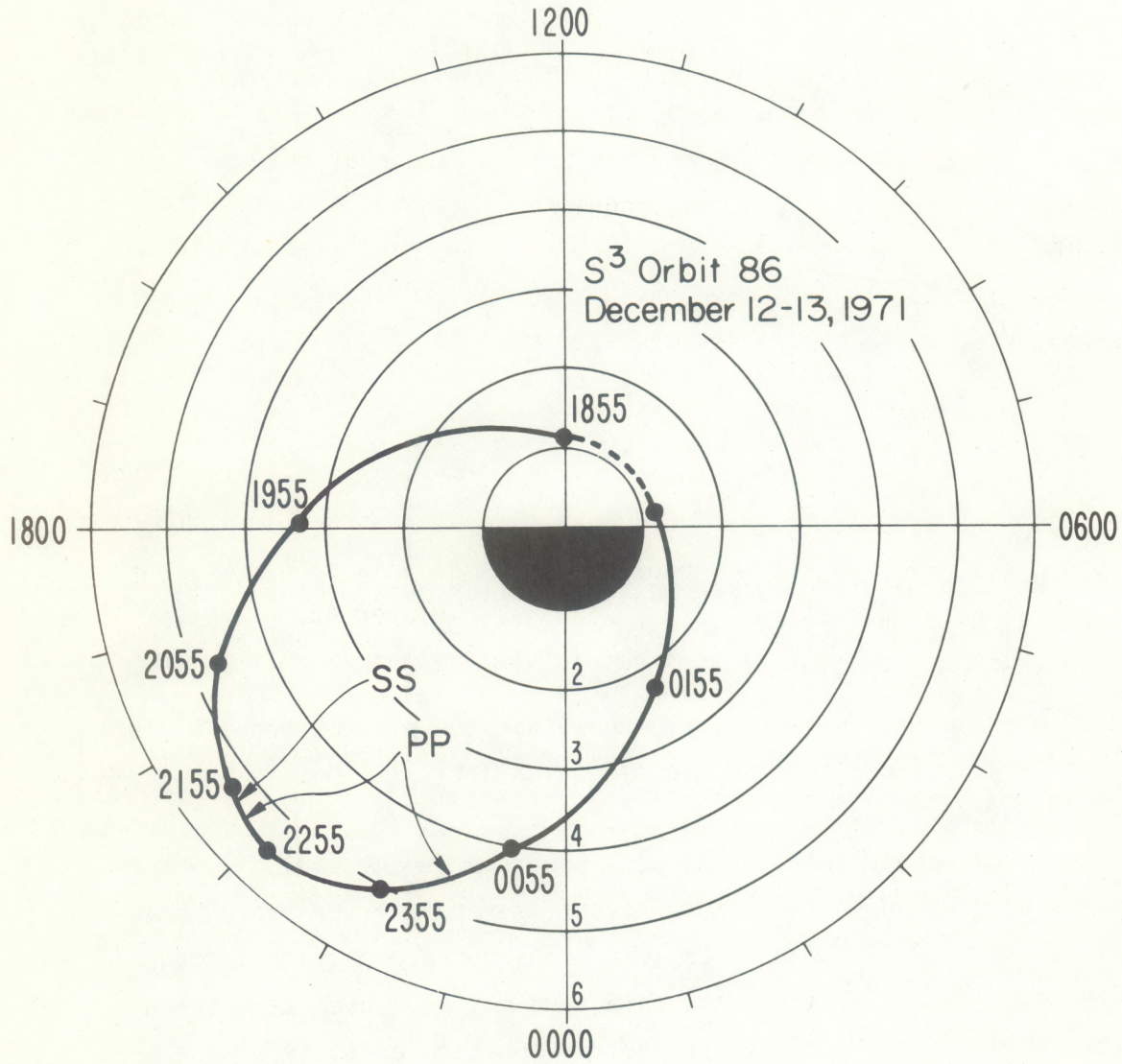

Figure 2. Explorer 45 (S^3) orbit during substorm. Plot gives L value in earth radii versus local time. UT is shown on orbit, and substorm start (SS) and plasmapause crossings (PP) are indicated.

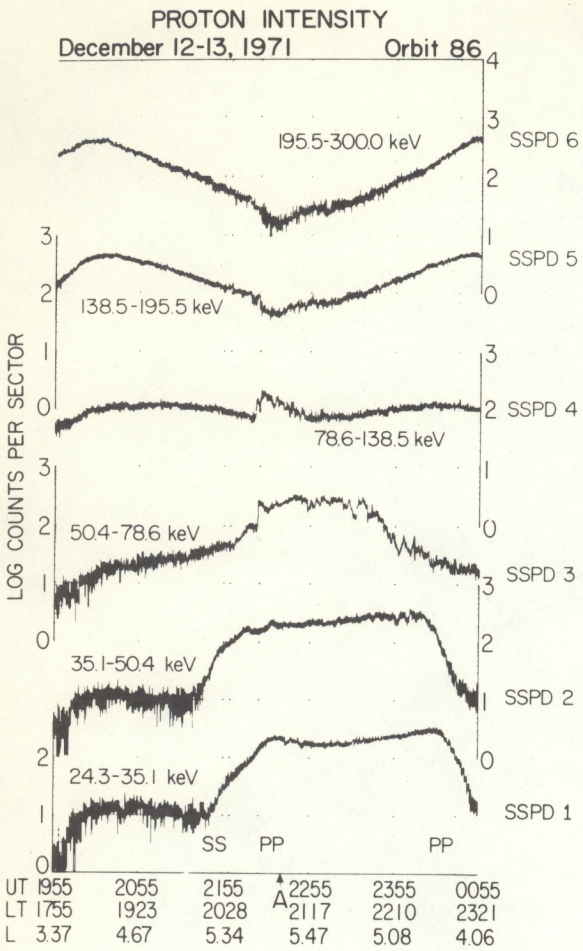

Figure 3. Response of Explorer 45 (S^3) solid-state detector proton channels for Orbit 86. Apogee (A) also shown. Local pitch angle of π/2 plotted. Spin period divided into 32 sectors with a sector being 0.264 sec.

3. Residual fluxes may remain from earlier substorm activity, which occurred approximately 3 hours before the one at 2200 UT ± 10 min.

Therefore, whenever the observations are within the plasmasphere, we feel that great care must be exercised in assigning arrival times to substorm-associated proton fluxes.

At approximately the time of peak substorm epoch, 2221 UT, a further increase occurred in the intensities of several of the proton channels. This was near the time of Explorer 45's outward passage through the plasmapause (fig. 3). This increase thus may have been associated with either plasmapause activity or further substorm activity at the height of the substorm. Note that the two high-energy channels in

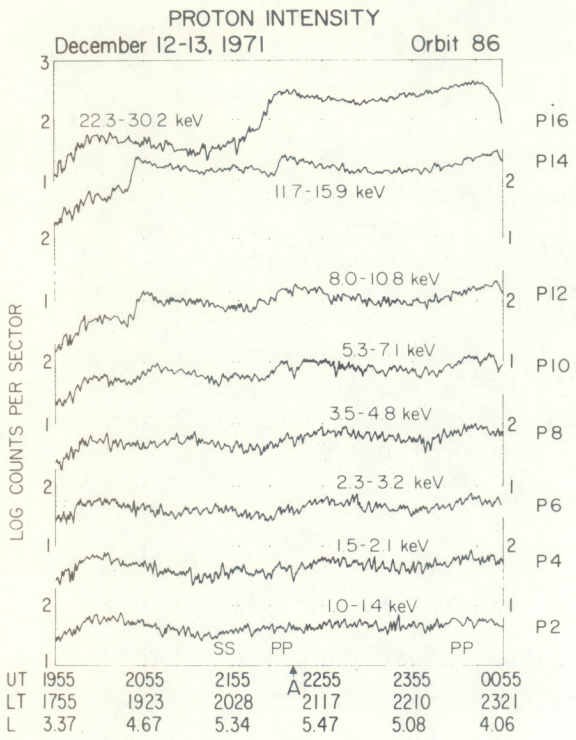

Figure 4. Response of Explorer 45 (S^3) electrostatic analyzer-channeltron proton channels for Orbit 86. Spin period divided into 32 sectors with a sector being 0.264 sec.

figure 4 show a small depression after the satellite exited the plasmapause. Figure 5, an expanded plot of this period, shows the 138.5 to 195.5 keV proton channel and a plot of the local magnetic field variation. Note that the two high-energy proton channels responsed adiabatically to the local B variations during the substorm.

To examine the spectral development of the proton distribution as the substorm progressed, we computed 5-min averages of the differential energy spectra during the interval of study (fig. 6). Spectra obtained before 2221 UT correspond to observations inside the plasmapause, after 2221 UT to those outside the plasmapause.

Figure 6 shows that before substorm onset a moderately deep trough at 30 to 50 keV was present in the spectrum, which agrees with earlier reports of proton spectra just inside the plasmapause (Williams et al., 1973), and that there was some evidence of possible residue fluxes due

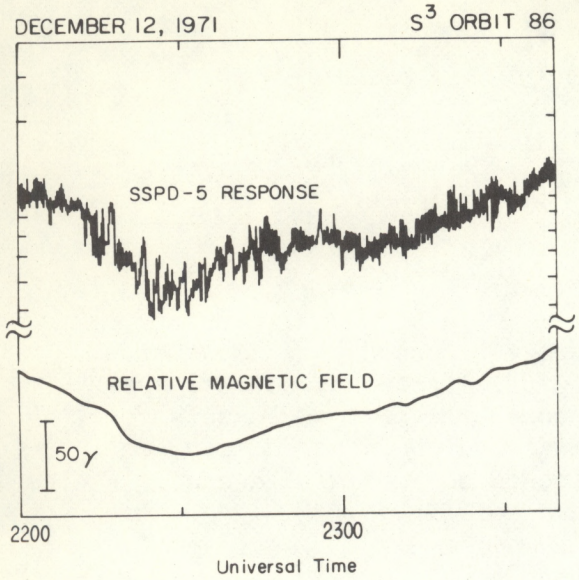

Figure 5. Solid-state proton detector channel 5 (138.5 to 195.5 keV) and relative magnetic field magnitude shown near and just after plasmapause exit. The tracking of these energetic proton intensities and the magnetic field indicates an adiabatic response at these energies during substorm peak epoch.

to previous activity. At onset, the trough started to fill-in reflecting the fact that the initial enhancement, as observed inside the plasmapause, was most rapid for 24.3 to 50.4 keV. Near substorm peak epoch, Explorer 45 exited the plasmapause and the spectrum filled-in across the trough. Although penetration into the plasmasphere modifies these proton intensities associated with the substorm, the expected energy dependence of this modification (Kennel and Petschek, 1966; Cornwall et al., 1970; Williams et al., 1973) leads us to believe that the narrow energy response during expansion either is a substorm parameter or is due to the filtering action of the $\overline{E}$ and $\overline{B}$ fields, and not caused by plasmasphere effects.

Figure 7 shows the energy density of the equatorially mirroring protons ($E_p \geq 1.01$ keV) through the substorm period and substorm onset and plasmapause encounter times. The spatial relation that these substorm associated protons have with the plasmapause appears similar to that of ring current protons and the plasmapause as reported by Frank (1971). This implies that these protons are simply the inward flow of the ring current protons in the combined geomagnetic and geoelectric fields. However, we shall see in the following sections that significant changes in presently published electric field models are required to explain both the proton and electron injections observed simultaneously by Explorer 45.

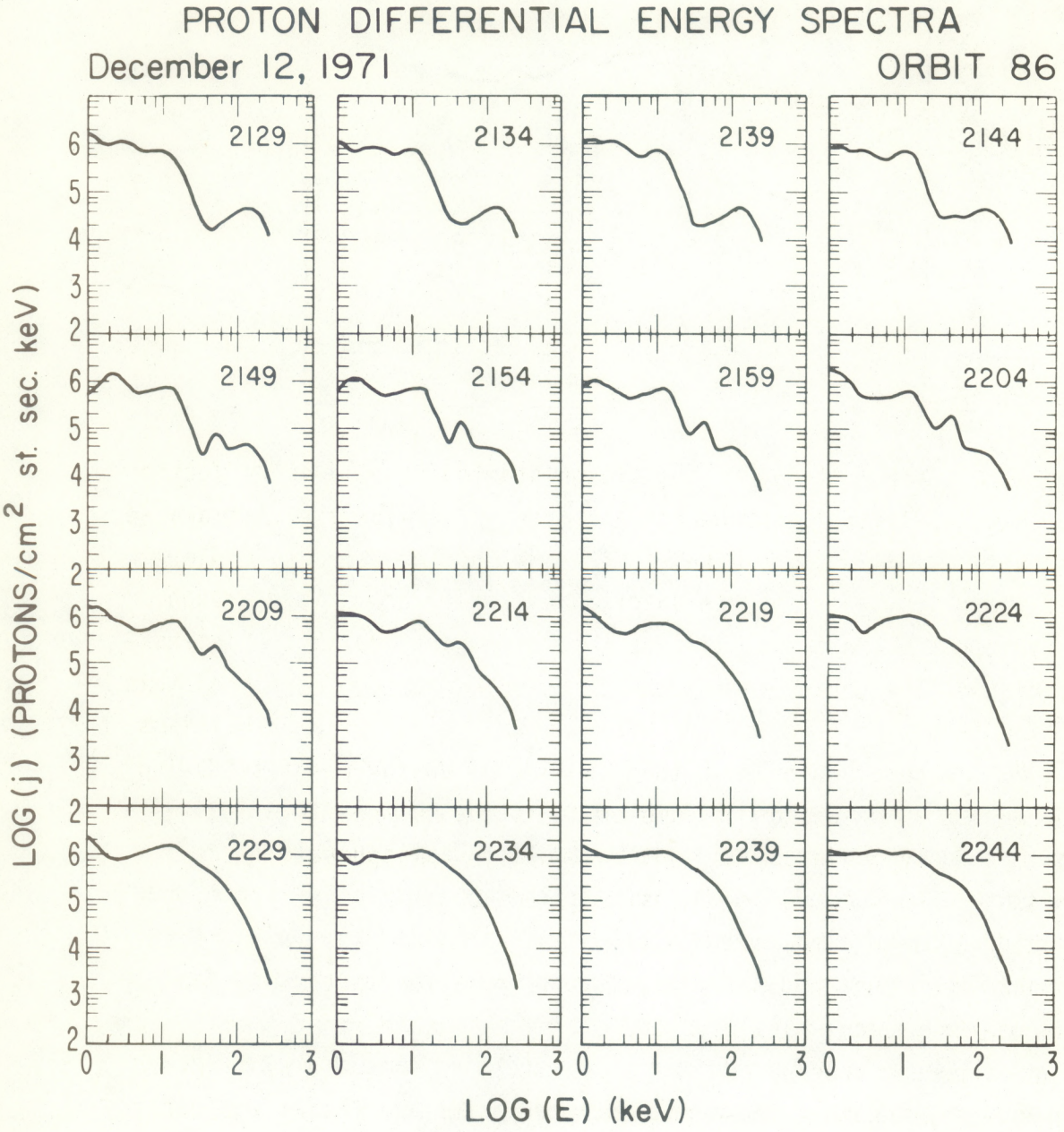

Figure 6. Five-minute averages of proton spectra taken before, during, and after the substorm of 2200 ± UT. Times are in UT. Explorer 45 exited the plasmasphere at ∿ 2221 UT.

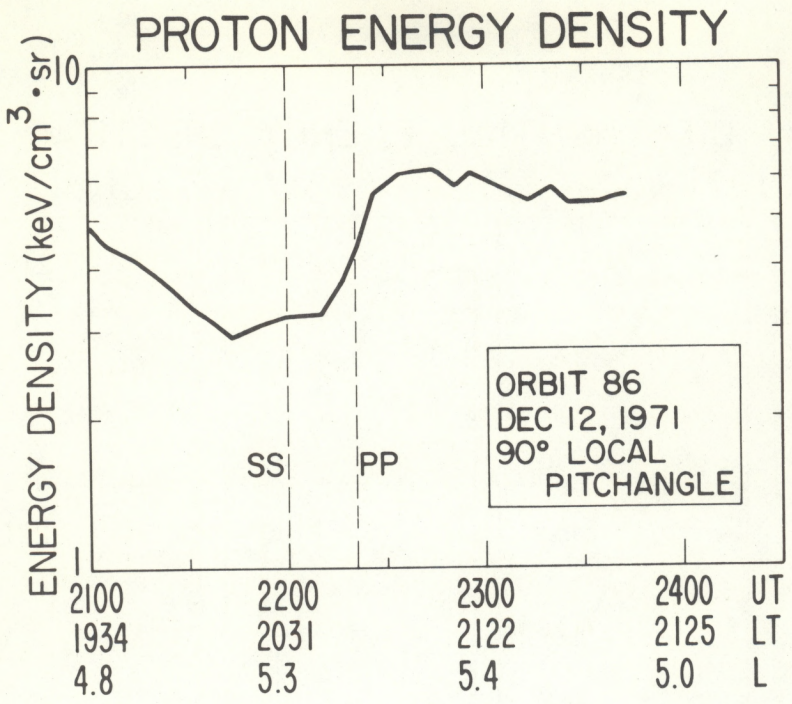

Figure 7. Proton energy density versus time.

2.3 Electron Observations

Figures 8 and 9 show the electron intensities for the period of interest. The electron energies shown are from 1.5 to 560 keV; this is a nearly continuous coverage except for a gap from 10.8 to 35 keV. This occurred because the satellite was in a telemetry sequence in which the lowest and the two highest energy channeltron channels were not sampled. In later orbits, the satellite data processor was reprogrammed so that all channels were sampled.

Table 1 shows our identification of the time when a particular electron channel showed a substorm associated intensity increase. Because the high-energy channels (fig. 8) are quite wide, we show the times for a given channel's initial increase (T_i), one-half maximum value ($T_{m/2}$), and maximum value (T_m). Although the low energy channels (fig. 9) are narrow enough to minimize timing problems, we show their T_i, $T_{m/2}$, and T_m for completeness. All the electron responses that we have associated

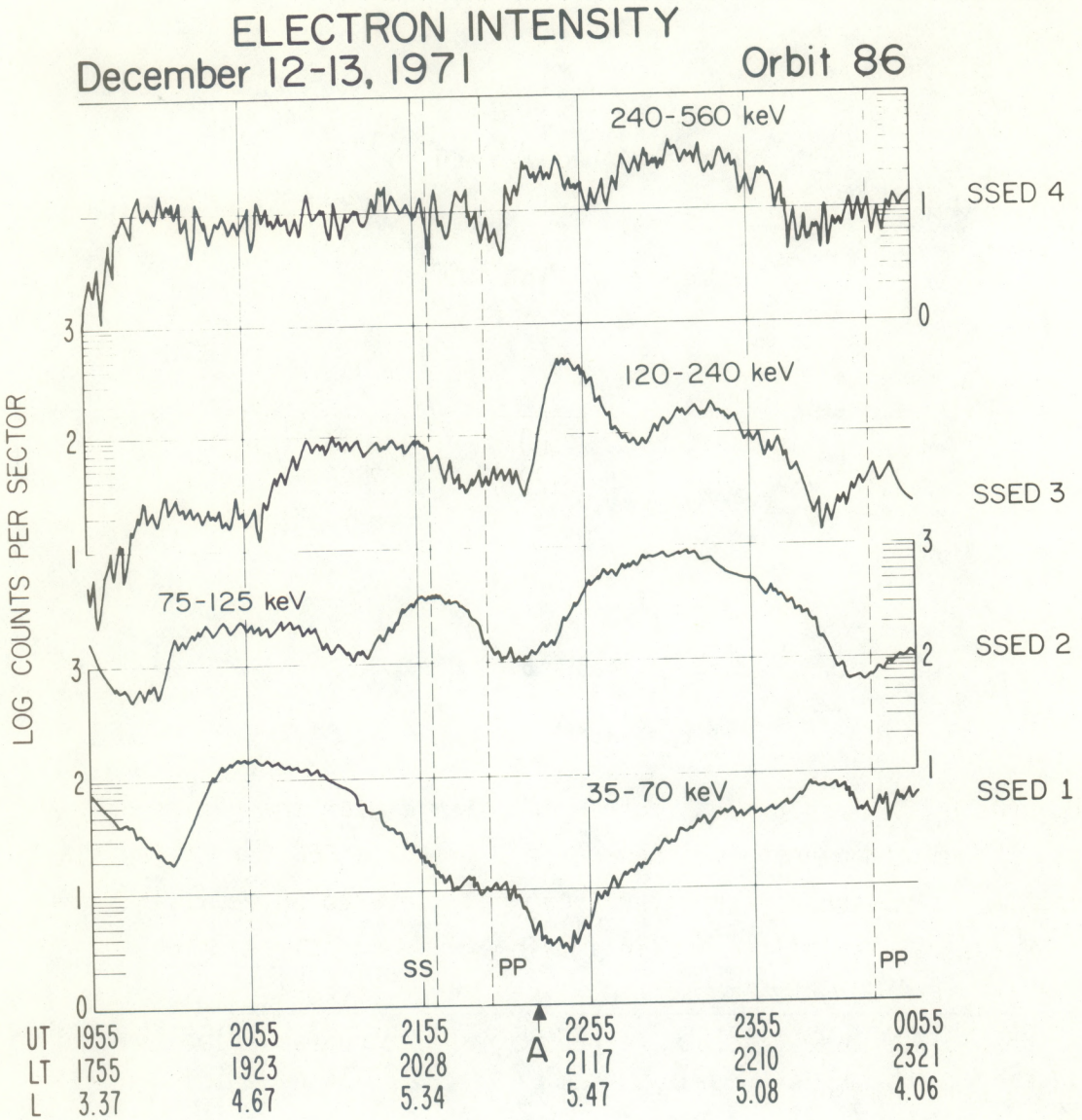

Figure 8. Response of Explorer 45 (S^3) solid-state detector electron channels for Orbit 86. Local pitch angle of π/2 plotted. Spin period divided into 32 sectors with a sector being 0.264 sec.

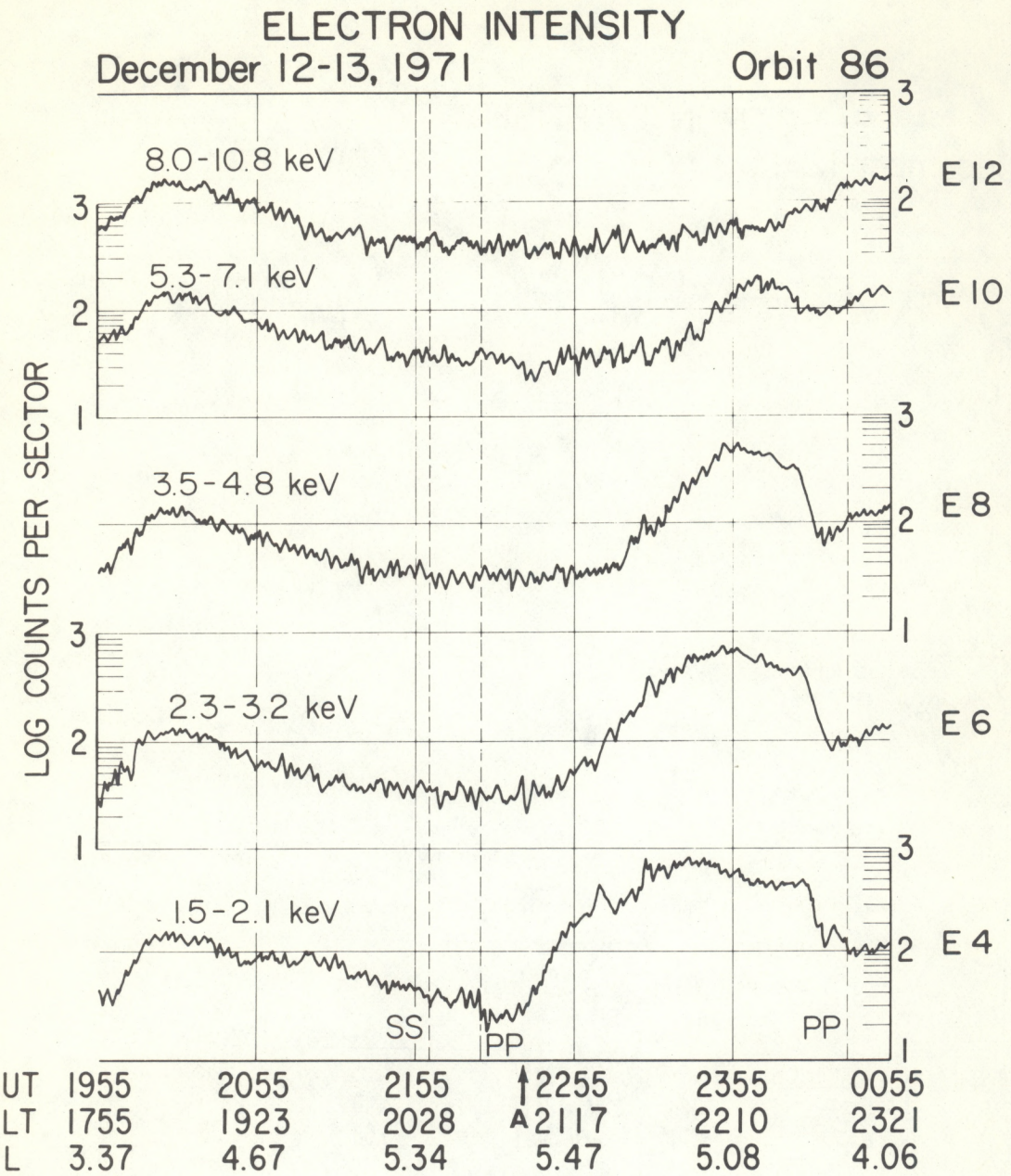

Figure 9. Response of Explorer 45 (S^3) electrostatic analyzer-channeltron electron channels for Orbit 86. Local pitch angle of $\pi/2$ plotted. Spin period divided into 32 sectors with a sector being 0.264 sec.

Table 1. Electron Response to Substorm at 2200 ± 10 UT.

E (keV)	T_i (UT)	$T_{m/s}$ (UT)	T_m (UT)
240 - 560	2228 ± 1	2230 ± 2	2242 ± 7
120 - 240	2234 ± 1	2243 ± 1	2247 ± 2
75 - 125	2239 ± 6	2255 ± 2	2329 ± 8
35 - 70	2250 ± 2	2325 ± 5	2347 ± 5
5.3 - 7.1	2339 ± 5	2350 ± 2	0007 ± 4
3.5 - 4.8	2314 ± 3	2342 ± 1	0000 ± 9
2.3 - 3.2	2253 ± 5	2332 ± 3	2354 ± 4
1.5 - 2.1	2230 ± 4	2312 ± 8	2339 ± 4

T_i = time of initital increase; $T_{m/2}$ = time of one-half maximum value; T_m = time of maximum value.

with the substorm at 2200 ± 10 UT occurred after the protons respond and outside the plasmasphere. Time dispersion effects thus should be unencumbered by plasmasphere effects.

Structure seen in figure 8 may be due to previous substorm activity. In addition, the 240 to 560 keV and 120 to 240 keV channels show peaks at ∿ 2330 UT and ∿ 2340 UT, respectively, which may be the second round trip for these electrons.

Figure 8 shows an energetic electron (35 to 560 keV) response time dispersion qualitatively consistent with localized injection away from the satellite with subsequent drift to the vicinity of Explorer 45. Similar drift time dispersion effects have been observed at synchronous altitudes (DeForest and McIlwain, 1971; Lezniak and Winckler, 1970).

Figure 9, however, shows the low-energy electrons (1.53 to 10.8 keV) displaying the opposite behavior, i.e., the lower energy channels show a substorm associated intensity increase earlier than higher energy channels.

This agrees with the synchronous altitude observations by Shelley et al. (1971), who interpret such substorm associated low-energy electron behavior as an earthward movement of the plasma sheet engulfing ATS-5.

The temporal development of the electron differential energy spectra, beginning just before the satellite encountered the plasmapause, is shown in figure 10. The missing data channels discussed earlier were filled in by interpolation. For electrons, the energy enhancement as observed by Explorer 45 was predominantly due to energies below $\sim$ 6 keV, and accordingly as the substorm injection progressed, the spectra became softer.

The energy density of the equatorially mirroring electrons ($E_e \geq 1.53$ keV) through the substorm period is shown in figure 11. Due to missing channels discussed earlier, we show the results of both a linear and log-log interpolation process in arriving at an estimate of the electron energy density. Note the exponential increase in electron energy density with time following the substorm and that the electron energy density is at most $\sim$ 1 percent of the proton energy density throughout this period.

ELECTRON DIFFERENTIAL ENERGY SPECTRA

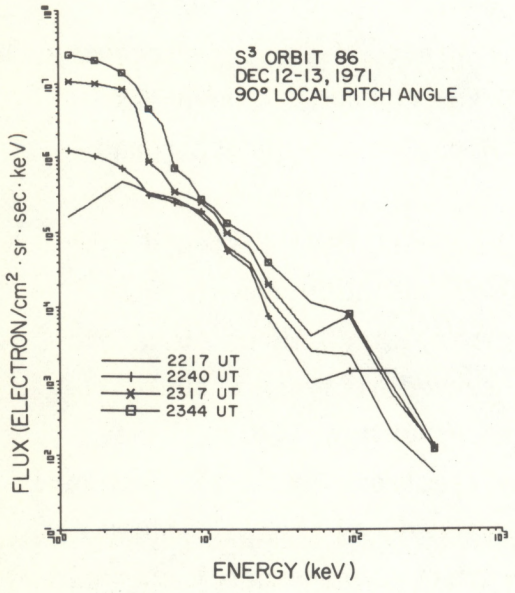

Figure 10. Electron spectra at various times during Orbit 86. 2217 UT = before electron substorm response and just prior to plasmapause exit. Remaining curves are at various phases of the substorm associated electron response and occur with Explorer 45 outside the plasmapause.

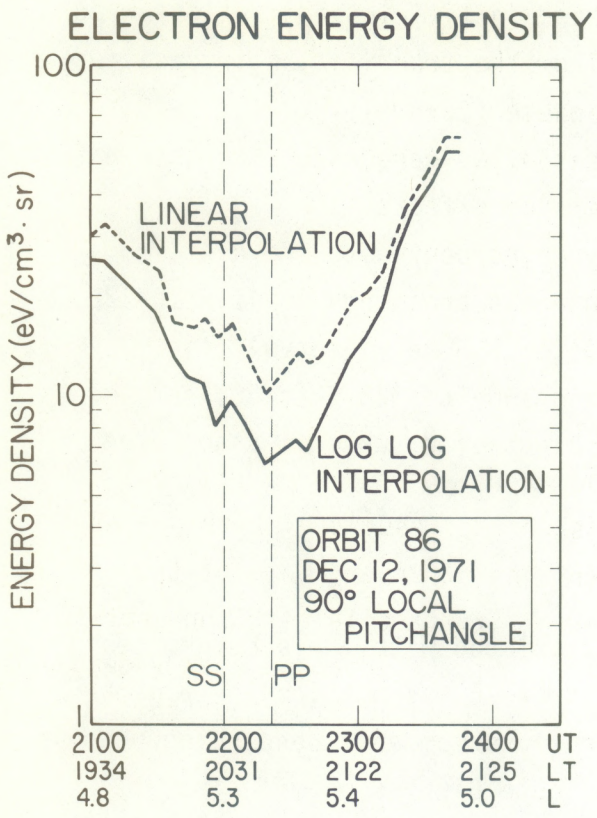

Figure 11. Electron energy density versus time. Results show both linear and log-log interpolation used to estimate energy density while including missing energy channels.

3. DISCUSSION

The results from this substorm suggest that the gross features of substorm particle signatures observed at geosynchronous orbit persist into the pre-midnight trapping region at least as deep as Explorer 45 apogee ($L \sim 5$ to 5.5). However, analysis of the detailed behavior of the proton and electron particle populations observed by Explorer 45 throughout this substorm points out small changes required in relating Explorer 45 and geostationary results *after* injection, using existing geomagnetic-geoelectric field models. We shall now summarize and discuss the proton results, the electron results, and the results of our attempts to explain the data via motion in combined electric and magnetic fields.

3.1 Protons

Enhanced proton intensities were present at the plasmapause very near substorm's onset (fig. 3). The local time was $\sim$ 2040 hours and the primary energy response during expansion phase occurred in the 24.3 to

50.4 keV interval (figs. 3 and 6). Because Explorer 45 was within the plasmasphere at the substorm's onset, these initial intensities observed may have been significantly attenuated from the true initial intensities by ion-cyclotron resonance at the plasmapause (Cornwall et al., 1970; Williams et al., 1973). For the same reason, we were unable to obtain a definitive measurement of energy dispersion effects.

By substorm peak-epoch and nearly coincident with the exit from the plasmapause, the major energy response had broadened to 11.7 to 138.5 keV with the major increases in the 22.3 to 78.6 keV interval (fig. 3). During this time, the high-energy proton channels (138.5 to 300 keV) displayed an adiabatic response with no signs of a substorm associated non-adiabatic response (fig. 5).

3.2 Electrons

Because the electron responses associated with the substorm beginning at 2200 ± 10 UT occurred while Explorer 45 was outside the plasmasphere and are thus unaffected by our previous comments concerning protons, we shall use the electron response to measure dispersion effects.

To see the entire Explorer 45 electron picture, we have plotted in figure 12 the arrival times listed in table 1 for all energies. Magnetic gradient drift curves in a dipole field are shown for reference.

A point should be made here about the use of T_i, $T_{m/2}$, and T_m. We have run a computer experiment that predicts the intensity versus time response of the Explorer 45 energetic electron detector assuming the injection of an energetic electron spectrum $E^{-\gamma}$ for n minutes Φ hours local time away from the satellite. Magnetic gradient drift is the only drift force employed. The results indicate that the most accurate timing is obtained from associating the time of the initial intensity increase, T_i, with the upper energy level of the channel. In contrast, the least accurate timing, due to a strong dependence on γ, n, and Φ, is the time of maximum value, T_m. The maximum value times show a strong tendency to yield travel times giving an injection region farther from the satellite than the true injection region. The use of $T_{m/2}$ has similar, although not

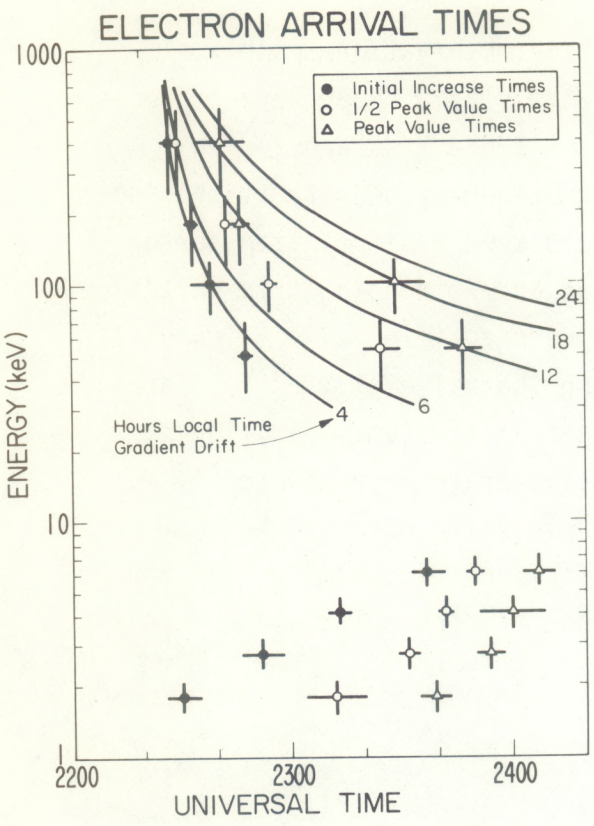

Figure 12. Energy versus T_i, $T_{m/2}$, and T_m. The T_i values are considered to yield most accurate energy-time dispersion curve.

pronounced, inaccuracies as T_m values. The T_m values of some of the Explorer 45 channels also may be further affected by plasmapause effects and by the radial dependence of normally existing fluxes.

These effects point out the difficulty in identifying the local time of injection and the width of the injection region by using only a single detector with wide energy bands. The indications for this substorm are that the energetic electron enhancement may have extended well into the dayside region.

It now remains for us to explain the appearance of the low-energy electrons at Explorer 45. We shall consider two cases: (A) the engulfing of Explorer 45 by the plasma sheet as it convects inward and (B) the formation of plasma clouds away from Explorer 45 and their detection by Explorer 45 due to the combined electric and magnetic fields.

Case A. The low-energy (1 to 10 keV) plasma sheet electrons are convected in via $\bar{E} \times \bar{B}$ drift and engulf Explorer 45. This explanation

has been used by Shelley et al. (1971) to explain their low-energy electron observations on ATS-5.

We can compare our low-energy electron observations with a simplistic view of what might be expected if the plasma sheet were to convect in and engulf Explorer 45. Vasyliunas (1968) has reported an exponential spatial structure in the electron energy density at the inner edge of the plasma sheet. If such a structure were simply transported inward past a quasi-stationary Explorer 45, an exponential time variation should be observed in the electron energy density (fig. 13). Figure 11 is consistent with this explanation. Using the value of $\sim e^{R/0.6}$ for inner edge plasma sheet energy density spatial structure (Vasyliunas, 1968) during substorm activity, where distances are in earth radii, we obtain from figure 11 an inward convection velocity of $\sim$ 1.7 km/sec. For $\gtrsim$ 200 γ, this implies a convection E field of $\sim$ 0.34 mV/m. If magnetic energy density controls the inner edge electron plasma sheet energy

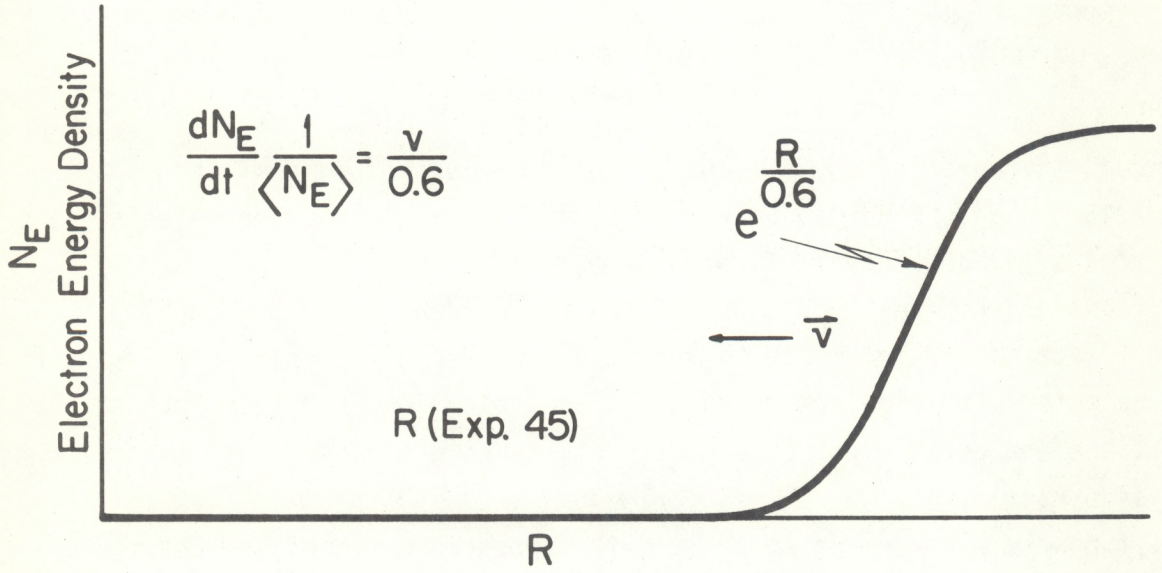

Figure 13. Schematic diagram showing simplified method of obtaining convective drift velocity, $\vec{v}$, at Explorer 45 altitudes assuming inward motion of an exponential plasma sheet inner edge energy density structure. This however does not yield a self-consistent picture for both electrons and protons.

density structure, and if the plasma sheet is adiabatically accelerated during convection then the fall off distance at 5.5 earth radii should be $\sim 0.2\ R_E$. Values for v and E are then $\sim$ 0.6 km/sec and $\sim$ 0.11 mV/m. Values in the above range also are obtained using the method of Shelley et al. (1971). With these values for $\bar{E}$, the plasma sheet is considered to convect earthward in a continuous manner from the geomagnetic tail to Explorer 45's position. We shall see this is inconsistent with flow in existing static $\bar{E}$ field models.

Case B. A plasma cloud forms east ofrExplorer 45, and the impact of the satellite with the plasma is governed solely by the combined electric and magnetic fields. In a *fixed* coordinate system, the satellite will never overtake the plasma for which

$$V_s = V_g + V_\varepsilon^{cr} + V_\varepsilon^{ext}$$

holds. Here V_s = satellite velocity, V_g = magnetic gradient drift velocity V_ε^{cr} = electric field drift velocity due to corotational component of $\bar{E}$, and V_ε^{ext} = electric field drift velocity due to "external" (non-corotational) $\bar{E}$ field. We use velocities in units of hours local time per/hour of universal time. Note that the electric field drifts considered here are produced by the radial component of $\bar{E}$.

In a coordinate system corotating with the earth $V_\varepsilon^{cr} \equiv 0$. Making this transformation, we have

$$V_s - V_\varepsilon^{cr} = V_g + V_\varepsilon^{ext} \ ;$$

V_ε^{cr} is obviously 1.0 hours LT/hour UT. During the substorm V_s = 0.82 hours LT/hour UT. This gives in a corotating coordinate system

$$-0.18 = V_g + V_\varepsilon^{ext} \ .$$

From our earlier discussion, with E in keV

$$V_g = -\frac{qE}{6} \text{ hours LT/hour UT at } L = 5.5 \ .$$

Thus for the electron portion of the plasma that is never seen by Explorer 45

$$-0.18 - \frac{E_s}{6} = V_\varepsilon^{ext} \ .$$

At the energy E_s, these electrons are stationary with respect to Explorer 45.

This energy can be estimated (fig. 13) by extrapolating the low- and high-energy electron time curves until they meet. A lower limit of 7 to 10 keV is obtained from the more accurate T_i curves. In addition, from figure 9 we see that the 8.0 to 10.8 keV channel shows no substorm associated response and thus can also be used as an estimate of E_s. Using $E_s \sim 9 \pm 2$ keV gives

$$V_\varepsilon^{ext} \approx -1.68 \pm 0.34 \text{ hours LT/hour UT} \ .$$

At $L = 5.5$ and $\vec{r}$ positive outward

$$E_r = -0.48\ V_\varepsilon \text{ mV/m} \ .$$

Thus for $E_s = 9 \pm 2$ keV

$$E_r^{ext} = 0.81 \pm 0.16 \text{ mV/m at } L = 5.5 \ .$$

In such a field, electrons of energy < 9 ± 2 keV are driven westward toward Explorer 45 and those > 9 ± 2 keV drift eastward. Eventually they would overtake the satellite.

The field ε_r^{ext} is that observed in a coordinate system corotating with the earth. It is important to specify the coordinate system simply for intercomparison. High altitude results (e.g., McIlwain, 1972) are usually given in a fixed system and low altitude results (Cauffman and Gurnett, 1972: Heppner, 1972; Maynard and Cauffman, 1973) in a system corotating with the earth.

It is difficult at best to compare high altitude results with low altitude observations, because of uncertainties in magnetic field-line mapping. Using a dipole magnetic field in the evening sector should give a lower limit to the value of the equatorial electric field projected to low altitude along the magnetic field line. Under such a projection, our inferred value of $\varepsilon_r^{ext} = 0.81 \pm 0.16$ mV/m transforms to a northward pointed electric field of magnitude ε_r^{ext} (low altitude) $\gtrsim$ 10 mV/m in the evening sector. However, because of the gross uncertainties in magnetic field-line mapping and the scarcity of published low altitude electric field values through the evening sector, we cannot determine whether this comparison represents a disagreement or an agreement between high and low altitude electric field observations.

To transform the Explorer 45 results to a fixed coordinate system, note that at L = 5.5

$$\varepsilon_r^{cr} = - 0.48 \text{ mV/m} .$$

Thus in a fixed coordinate system, the field observed becomes

$$\varepsilon_r^{F} = \varepsilon_r^{ext} + \varepsilon_r^{cr} = 0.81 \pm 0.16 - 0.48$$

$$\varepsilon_r^{F} = 0.33 \pm 0.16 \text{ mV/m} .$$

An analysis of ATS-5 data (McIlwain, personal communication) during this substorm yields a value of

$$\varepsilon_e^F = 0.0 \pm 0.03 \text{ mV/m}$$

at L = 6.8 and 1700 hours LT

or $$\varepsilon_r^{ext} = 0.32 \pm 0.03 \text{ mV/m}$$

3.3 Electric Field Model

The arrival of protons at Explorer 45 before the electrons is qualitatively consistent with the inward convection of a high altitude plasma sheet consisting of a proton and electron component. In its ambient position, such a plasma sheet in the geomagnetic tail is expected to have the positive ion component extend to lower altitudes than the negative electron component (Kennel, 1969). The energy density profiles (fig. 7 and 11) are also consistent with inward convection of a high altitude plasma sheet.

However, to become more quantitative and attempt to evaluate the above alternatives, we have compared our results with flow patterns expected from a model geomagnetic-geoelectric field constructed specifically to explain particle signatures observed at ATS-5 in geostationary orbit (McIlwain, 1972). Note that this is a *fixed* coordinate system.

Proton and electron trajectories in the McIlwain model are shown in figures 14 and 15. The proton trajectories are for all values of magnetic moment that are able to reach Explorer 45 in this model and thus contribute to the observed energy response. Trajectories are shown for total energy, $T \equiv E + \Phi$ = constant, curves. Here Φ = electric potential and E = particle energy. The different shading represents different values of μ (the magnetic moment), and the boundaries of each shaded region are labeled with the value of the total energy. The region of Explorer 45 observations is the darkened area at L $\sim$ 5 to 5.5 and 2030 to 2230 LT. As shown in figure 14, protons in a wide energy band ($\sim$ 5 to 100 keV) are predicted where the substorm proton responses were actually observed. They would come from the regions in the geomagnetic tail indicated in figure 14 and would pass through geostationary orbit near midnight. Thus, the proton observations during the substorm are quantitatively consistent with the McIlwain model.

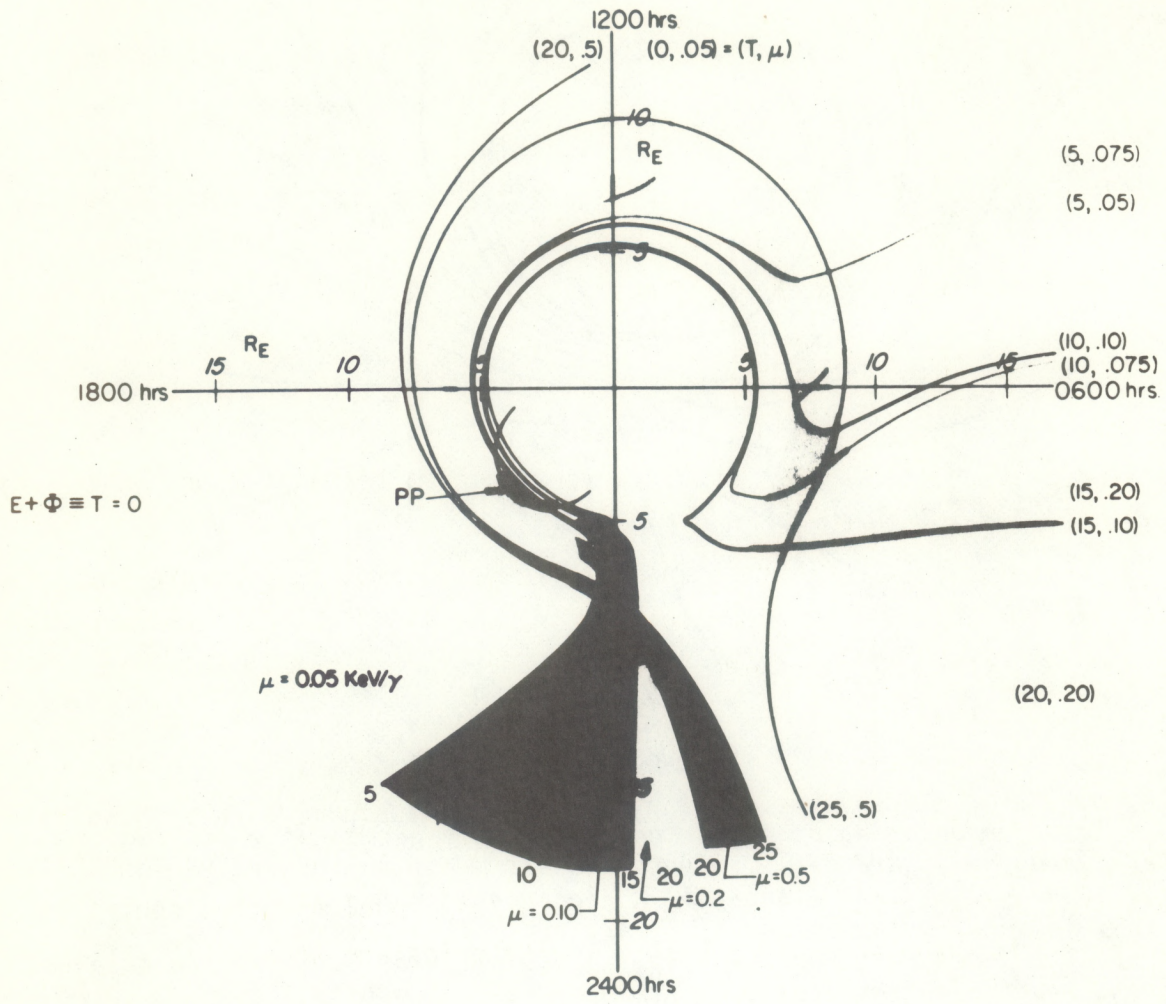

Figure 14. Local time versus altitude plot showing trajectories of all particles capable of reaching Explorer 45 and producing observed energy response. Trajectories calculated using the combined geomagnetic-geoelectric field constructed by McIlwain (1972) to explain particle signatures at geosynchronous orbit. Shaded regions in geomagnetic tail correspond to various values of the particle magnetic moment, μ. They are bounded by trajectory curves identified by constant total energy $T = E + \Phi$ where E = particle kinetic energy and Φ = electric potential. Explorer 45 orbit shown with plasmapuse exit (PP) and region of substorm observations (shaded portion of orbit). The protons come from a wide region in the geomagnetic tail.

However, in terms of continuous flow from the geomagnetic tail, it does not seem possible for this same model to explain the simultaneous

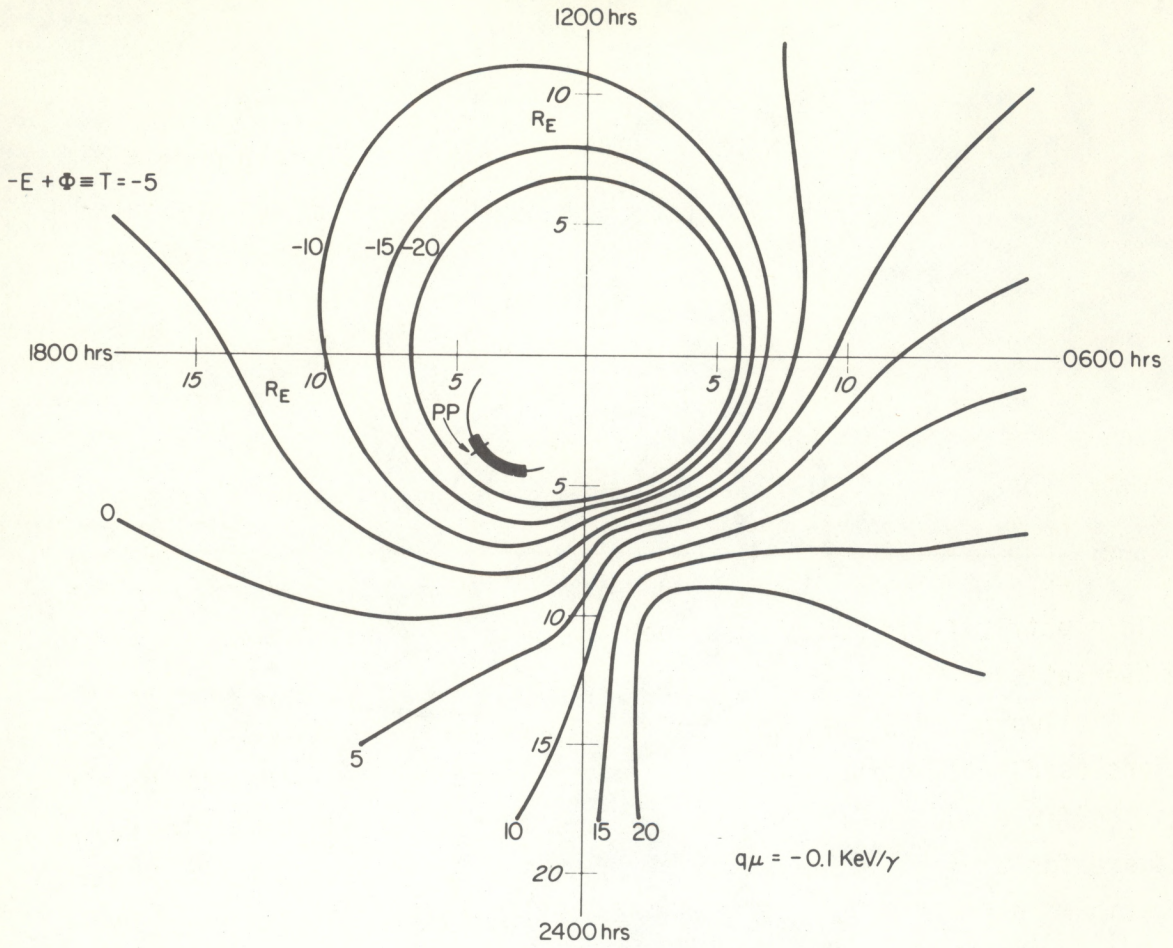

Figure 15. Trajectories of electrons in the same geomagnetic-geoelectric field used for figure 14. Trajectories shown for various values of total energy T = - E + Φ and for an electron magnetic moment of μ = - 0.1 keV/γ. Several other values of μ were run with the same result — this particular geomagnetic-geoelectric field configuration is unable to cause plasma sheet electrons to reach Explorer 45 at L = 5 to 5.5 and 2030 to 2230 hours LT.

electron observations. Figure 15 shows trajectories of electrons with magnetic moments of - 0.1 keV/γ in the model fields. Note that the entire orbit of S^3 is within the region defined by *closed* electron trajectories. Trajectories were computed for electrons over a wide range of magnetic moments and initial total energies, and the results were similar to those shown in figure 15; i.e., electrons originating in the geomagnetic tail could *not* reach Explorer 45's position in this model field via a continuous flow process.

Therefore, we feel that existing static electric field models are unable to explain the injection of substorm protons and electrons into the evening sector at equatorial altitudes of $\sim$ 5 to 5.5 R_E. A discontinuous change when the substorm starts is apparently required to explain the sudden appearance of these particles at altitudes well within the geostationary orbit. Perhaps a short-lived change in the direction and magnitude of the electric field is sufficient for this injection. However, perturbations in the magnetic field may also be important in determining substorm particle observations.

After the plasma cloud is injected to low altitudes, drift in the static electric field model does seem to explain the subsequent Explorer 45 observations.

McIlwain (1972) has carefully outlined the assumptions and simplifications used in constructing this electric field model. Of importance is that the field model pertains to K_p values of $\sim$ 1, while the Explorer 45 data are for K_p = 3. However, the above results indicate that small modifications in field direction at L $\sim$ 5.5 might be made to the model geomagnetic-geoelectric field in order to better fit the Explorer 45 observations. As discussed earlier, the proton responses are consistent with the model field, and quaulitatively, at least, the electrons can be explained by a small (0.33 $\pm$ 0.16 mV/m) outward radial component of the everning sector electric field in a fixed coordinate system.

We therefore favor alternative B discussed above as the preferred explanation to the responses associated with the simultaneous proton and electron substorm as observed by Explorer 45 at 5 to 5.5 earth radii and 2030 to 2230 hours LT. This agrees with the plasma cloud concepts advanced by DeForest and McIlwain (1971).

4. CONCLUSIONS

In summary, the Explorer 45 observations reported here indicate that the gross features of the substorm signature persist deep into the nightside trapping region. However, detailed analysis shows that the static

electric field model derived from geostationary observations is unable to explain the injection of substorm associated particle intensities observed by Explorer 45 at 5 to 5.5 R_E and 2030 to 2230 hours LT. However, the model does seem to explain observations obtained after the initial particle injection. To best fit the Explorer 45 observations, we obtain an outward electric field component of magnitude $\sim 0.81 \pm 0.16$ mV/m in a corotating coordinate system ($\sim 0.33 \pm 0.16$ mV/m in a fixed coordinate system).

5. ACKNOWLEDGMENTS

We gratefully acknowledge Drs. N. Maynard, R. Hoffman, and L. Cahill for use of data that made this study possible. Discussions with Drs. H. Sauer, N. Maynard, G. Reid, and T. Holzer, as well as extended discussions and correspondence with Dr. C. E. McIlwain and the use of unpublished ATS-5 results have all ben very valuable in this study. The ground magnetic records were supplied by the National Geophysical and Solar-Terrestrial Data Center, Boulder, Colorado. This work was performed in part under NASA contract S-50028.

6. REFERENCES

Akasofu, S.-I. (1968), Polar and Magnetospheric Substorms (D. Reidel, Dordrecht, Netherlands), p. 22.

Arnoldy, R. L., and K. W. Chan (1969), Particle substorms observed at the geostationary orbit, *J. Geophys. Res.*, *74*, p. 5019.

Cauffman, D. P., and D. A. Gurnett (1972), Satellite measurements of high latitude convection electric fields, *Space Sci. Rev.*, *13*, p. 369.

Cornwall, J. M., F. V. Coroniti, and R. M. Thorne (1970), Turbulent loss of ring current protons, *J. Geophys. Res.*, *75*, p. 4699.

DeForest, S. E., and C. E. McIlwain (1971), Plasma clouds in the magnetosphere, *J. Geophys. Res.*, *76*, p. 3587.

Frank, L. A. (1971), Relationship of the plasma sheet, ring current, trapping boundary, and plasmapause near the magnetic equator and local midnight, *J. Geophys. Res.*, *76*, p. 2265.

Heppner, J. P. (1972), Electric field variations during substorms: OGO-6 measurements, *Planet. Space Sci.*, *20*, p. 1475.

Kennel, C. F. (1969), Consequences of a magnetospheric plasma, *Rev. Geophys.*, *7*, p. 379.

Kennel, C. F., and H. E. Petschek (1966), Limit on stably trapped particle flux, *J. Geophys. Res.*, *71*, p. 1.

Lezniak, T. W., and J. R. Winckler (1970), Experimental study of magnetospheric motions and the acceleration of energetic electrons during substorms, *J. Geophys. Res.*, *75*, p. 7075.

Maynard, N., and D. P. Cauffman (1973), Double floating probe measurements on S^3, *J. Geophys. Res.*, in press.

McIlwain, C. E. (1972), "Plasma convection in the vicinity of the geosynchronous orbit." *Earth's Magnetospheric Processes*, ed. B. M. McCormac (D. Reidel Pub. Co.), p. 268.

Parks, G. K., and J. R. Winckler (1968), Acceleration of energetic electrons observed at the synchronous altitude during magnetospheric substorms, *J. Geophys. Res.*, *73*, p. 5786.

Shelley, E. G., R. G. Johnson, and R. D. Sharp (1971), Plasma sheet convection velocities inferred from electron flux measurements at synchronous altitude, *Radio Sci.*, *6*, p. 305.

Smith, P. H., and R. A. Hoffman (1973), Energy dependent inner boundaries of ring current particles observed at the beginning of magnetic storms, Preprint, Goddard Space Flight Center, June 1973. Also presented at Chapman Memorial Symposium, Boulder, Colorado, June 1973.

Vasyliunas, V. M. (1968), A survey of low-energy electrons in the evening sector of the magnetosphere with OGO 1 and OGO 3, *J. Geophys. Res.*, *73*, p. 2839.

Williams, D. J., T. A. Fritz, and A. Konradi (1973), Observations of proton spectra ($1.0 \leq E_p \leq 300$ keV) and fluxes at the plasmapause, *J. Geophys. Res.*, in press.

Winckler, J. R. (1970), "The origin and distribution of energetic electrons in the Van Allen radiation belts." *Particles and Fields in the Magnetosphere*, ed. B. M. McCormac (D. Reidel Pub. Co.), p. 332.